Journal of Nanostructure in Chemistry (2023) 13:497–505
https://doi.org/10.1007/s40097-022-00478-1

ORIGINAL RESEARCH

Modeling phosphorene and MoS_2 interacting with iron: lubricating effects compared to graphene

Gabriele Losi[1] · Michele Cutini[1] · Paolo Restuccia[2] · M. Clelia Righi[1]

Received: 11 November 2021 / Accepted: 14 February 2022 / Published online: 2 March 2022

Abstract

Phosphorene, a single layer of black phosphorus, is attracting interest for several applications, among which tribology. Here, we investigate its possible use as a solid lubricant for iron-based materials by comparing its friction-reduction properties with MoS_2 and graphene. Through first-principle calculations, we predict that phosphorene adheres more strongly to the native iron surface than the other considered 2D materials. The higher adhesion suggests that a stable and durable coverage of reactive surface regions can be obtained with phosphorene. Furthermore, our simulation uncovers the peculiar behavior of phosphorene to exfoliate into two atomic-thin layers upon interface intercalation. This capability makes phosphorene reduce the nano-asperity adhesion very efficiently thanks to the simultaneous passivation of the surface and countersurface. These results suggest that better performances could be obtained by phosphorene than other solid lubricants at low concentrations.

Keywords Phosphorene · Friction · Adhesion · Interfaces

Introduction

According to the International Energy Agency, the most impacting technologies to reduce CO_2 in the near future should be related to end-use energy efficiency [1]. It has been estimated that 23% of the world's total energy consumption is due to friction, and this considerable energy waste can be reduced up to 40% in the next 15 years by improving the tribology technologies. Nowadays, these technologies are based on materials; thus, the design and development of lubricant and coatings to reduce friction and wear in machine components is of paramount importance for energy efficiency and CO_2 emission reduction on a global scale [2].

Two-dimensional (2D) materials, thanks to the weak interlayer interaction and surface chemical stability, present exceptional lubricant properties. In recent years, significant advances have been made in the scientific research and industrial applications of 2D materials on metallic substrate, for anti-friction, anti-wear, and energy storage applications [3–5].

Among the most recently considered 2D materials, phosphorene—a single layer of black phosphorus [6–10]—has shown very promising properties for reducing friction. Superlubricity has been observed using treated black phosphorus nanosheets in an aqueous solution for a wide range of sliding velocities, additive concentrations, and applied pressures [10]. Even if phosphorene flakes undergo ambient degradation, they seem to maintain their lubricating properties [7] thanks to the strong interactions between P–OH groups and water molecules [6]. Superlubricity of phosphorene has also been identified at the nanoscale, where a perpendicular orientation of the layers has been shown to reduce the interlayer-binding energy and the shear strength by one order of magnitude compared to the standard layer orientation [11]. Phosphorus is also a key element for extreme-pressure additives included in the engine oils. As shown by in situ spectroscopy analysis, the capability of organophosphorus additives to reduce the friction coefficient of steel-on-steel is related to the tribologically induced formation of iron phosphite [12, 13]. The P-rich tribofilm is formed thanks to the release of elemental phosphorus by the dissociative chemisorption of the molecules [13], promoted by the tribological conditions, as shown by *ab initio*

✉ M. Clelia Righi
clelia.righi@unibo.it

[1] Department of Physics and Astronomy, University of Bologna, Viale Carlo Berti Pichat 6/2, 40127 Bologna, Italy

[2] Department of Chemistry, Imperial College London, 82 Wood Lane, London W12 0BZ, UK

molecular dynamics simulations [14, 15]. The lubricating effect of adsorbed phosphorus resides in its ability to form P–P bonds that reduce the reactivity of the iron substrate, especially at high coverage [16].

The above findings suggest that phosphorene may be a good lubricant for steel. Here, we use first-principles calculations to explore the capability of phosphorene to chemisorb on iron and reduce its adhesion and friction. A similar analysis is performed for MoS_2, a well-known solid lubricant, which can also lubricate steel as a product of tribochemical reactions involving lubricant additives, such as molybdenum dithiocarbamates [17–19].

We compared the results with the lubrication of graphene, which we have previously shown to be able to reduce iron adhesion and shear strength efficiently [20, 21], in agreement with the experimental evidence [22–24].

Using density functional theory (DFT) calculations, we show that phosphorene chemisorbs on iron more strongly than MoS_2 and graphene [21]. Moreover, phosphorene can outperform these two well-established solid lubricants at low coverage conditions. The reason resides in the ability of the single phosphorene layer to split into two separate atomic planes once intercalated at the iron interface. Such peculiar behavior, governed by the interplay between the Fe–P and P–P interactions, is particularly advantageous for obtaining the simultaneous passivation of the substrate and the countersurface, with a consequent drop of adhesive friction.

Method

We performed DFT simulations employing the Quantum Espresso software [25, 26]. The electronic wave functions are expanded on a plane-wave basis set, and we used ultrasoft pseudopotentials to describe the ionic species, including the core electrons [27]. We employed the generalized gradient approximation (GGA) within the Perdew–Burke–Ernzerhof (PBE) parameterizations as exchange-correlation functional [28]. We took into account London dispersion forces by adopting the D2 scheme [29], using the value for the s_6 scaling factor suggested in the original paper ($s_6 = 0.75$). This type of dispersion scheme gave very good results for computing not only organic [30–34] but also inorganic materials properties [35, 36]. Recent investigations indicate that more modern dispersion correction schemes are also appropriate for simulating the chemisorption of 2D material on metal and ceramic surfaces [37, 38]. However, in the present case, the interaction of the three considered layered materials and iron is chemical, not physical. Furthermore, PBE-D2 provides a good description of black phosphorus and phosphorene interlayer energy [39]. Previous studies performed in our group regarding the tribological properties of graphene and transition metal dichalcogenides demonstrated that PBE-D2 could accurately describe interlayer sliding properties [11, 21, 40–42]. For the phosphorene on iron, the kinetic energy cut-off to expand the wave function and the charge densities were 30 Ry and 240 Ry, respectively. Instead, for MoS_2 on iron, the cut-off values were set to 40 Ry and 320 Ry, respectively. All the different systems were constructed with at least 15 Å of vacuum between vertical replicas.

We considered the (110) Fe surface, which is the most stable surface of iron [21, 43, 44]. The adopted unit cell is orthorhombic with cell vectors equal to a and $\sqrt{2}a$, where a is the iron bulk lattice parameter (body-centered cubic unit cell) relaxed at the PBE-D2 level (a=2.85 Å). We took into consideration supercells to reduce the mismatch between 2D materials and iron. The layer material is slightly deformed to fit into the considered supercell, whereas the Fe lattice is kept at equilibrium. For matching phosphorene and iron, a $3 \times 4\sqrt{2}$ iron supercell and a 2×5 phosphorene supercell were adopted, where the mismatch between iron and phosphorene is 2.6% and 2.3% for the a and b cell vectors. A $2 \times 4\sqrt{2}$ iron supercell is instead adopted for iron for matching a $\sqrt{3} \times 5$ MoS_2 supercell with a corresponding mismatch of 2.9% and 1.8% along the sides of the supercell. The iron surface is simulated using two layer-thick slabs (one A–B Fe layer) to reduce the computational costs as much as possible. This model simplification, already adopted in previous calculations [45], is dictated by the computational cost of the presented calculations. The small energy difference observed when considering two layers instead of three is just a limited fraction (~2%) of the actual phosphorene chemisorption energy, which fully justifies the presented approach (see supporting information).

The iron interfaces were constructed using the same supercells adopted for the surface calculations. In this case, we included two iron slabs in the supercell. One or two layers of the 2D material were intercalated within the iron slab, depositing each layer at an initial distance of 1.5 Å from the metal surface. The interface geometry was then allowed to relax to the equilibrium configuration. MoS_2 presents two possible different equilibrium stacking [40]. In the current work, the 2L-R0 stacking was adopted. We also evaluate the potential energy surfaces (PES) of the different sliding interfaces. It describes the adhesion energy between two surfaces in contact as a function of their relative lateral position, $\gamma(x, y)$. The PES is calculated by shifting the upper surface to different lateral positions with respect to the lower surface, defining a grid of points with ~0.7 Å spacing along the x- and y-directions. The equilibrium separation between the layers is obtained for every lateral position by optimizing the z degree of freedom while keeping the x and y coordinates fixed. The PES is calculated by interpolating the adhesion energies at each grid point with radial basis functions [43, 46]. On top of the PES, we can estimate the

minimum energy path (MEP) connecting the PES minima passing through saddle points, which constitutes the most favorable sliding path. The ideal shear strength is then calculated along the MEP [47]. The latter estimates the maximum shear resistance and is strictly connected to the static friction of the sliding interface. We computed the MEP with the simplified string method [48], as implemented in a workflow for throughput interfaces developed by our group [43, 46]. To understand the connection between adhesive friction and interfacial electronic properties, we evaluate the charge redistribution occurring in the interfacial region, as described in Ref. [19] and later in the text. The charge redistribution is normalized by the average number of electrons per atom to compare different systems.

Results and discussion

Chemisorption of phosphorene and MoS_2 on iron

The first step in our analysis is evaluating the adhesion of each 2D material to the metallic substrate. To this aim, we have deposited one layer on the Fe(110) surface at an initial distance of 1.5 Å. After the structural optimization, the adhesion of the layer to the metallic substrate is evaluated as

$$E_{adh} = \left(E_{tot} - E_{layer} - E_{iron}\right)/A, \quad (1)$$

where E_{tot} is the energy of the adsorbate system, while E_{layer} and E_{iron} are the energies of the isolated layer and the substrate, respectively, and A is the in-plane area of the supercell. Figure 1 shows the optimized structures.

The calculated binding energies and distances reported in the picture indicate that phosphorene strongly chemisorbs on iron, with the adhesion energy about three times larger than graphene, which is −0.89 J/m^2. The stronger chemisorption of phosphorene compared to graphene on transition metals surfaces has also been observed in Ref. [49]. We noticed that upon adsorption, the distance between the two atomic planes forming the phosphorene increases by 4.7% with respect to its value in the isolated layer, thus indicating the strong interaction between the layer and the substrate weakens the intralayer interaction. The adhesion energy of MoS_2 is in-between those of graphene and phosphorene, i.e., −1.60 J/m^2. For this material, its structure is preserved with a vertical expansion of just 0.6% compared to the isolated layer.

Intercalation of phosphorene and MoS_2 at the iron interface, a comparison with graphene

The adhesion energies of phosphorene and MoS_2 on iron indicate that both the materials can adhere to the native iron surface and resist the peeling-off by a rubbing countersurface better than graphene. As a next step, we evaluated the friction-reduction capability of the thin coatings. Therefore, we constructed an interface composed of two iron slabs, which mimics a nano-asperity contact, and calculated the interfacial adhesion both in the absence and in the presence of intercalated layers. In the latter, we first covered the substrate and then the whole metallic interface. In Fig. 2, we show the optimized structures of the considered interfaces, where the results previously obtained for graphene [21] are also shown for comparison. A summary of the calculated data is also reported in Table 1 and Fig. 3.

The adhesion energy calculated for the most stable configuration of the clean iron interface, corresponding to the bulk stacking sequence, is −4.6 J/m^2, i.e., twice the energy of the Fe(110) surface. The intercalation of a layer of a 2D material produces a reduction of the adhesion energy; see Table 1 and Fig. 3. Interestingly, when a phosphorene single layer is intercalated at the iron interface, it spontaneously dissociates into two thin atomic planes that simultaneously passivate the two iron surfaces in contact; see Fig. 2c. Therefore, the adhesion energy between the two P-saturated iron surfaces becomes as low as −0.6 J/m^2, corresponding to one-eighth of the adhesion energy between two pristine iron slabs. This dramatic decrease is linked to the ability of

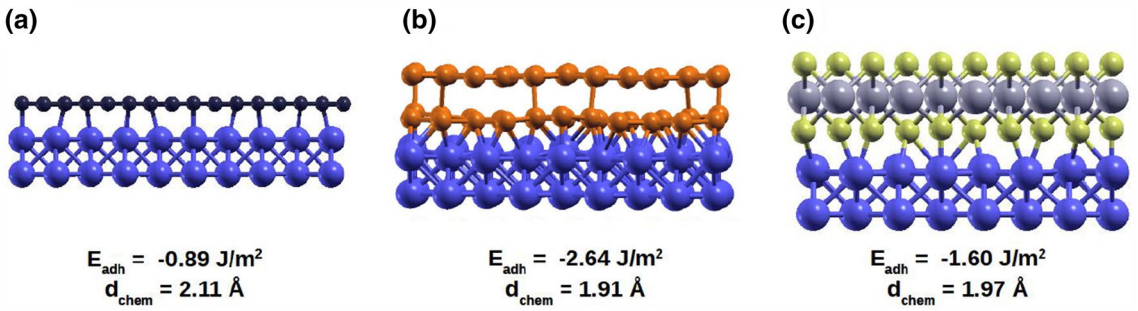

Fig. 1 Binding geometries of graphene (**a**), phosphorene (**b**), and MoS_2 (**c**) on native Fe(110) surface. The equilibrium chemisorption distance, d_{chem}, is defined as the distance from the bottom atomic plane of each 2D layer to the underlying iron substrate

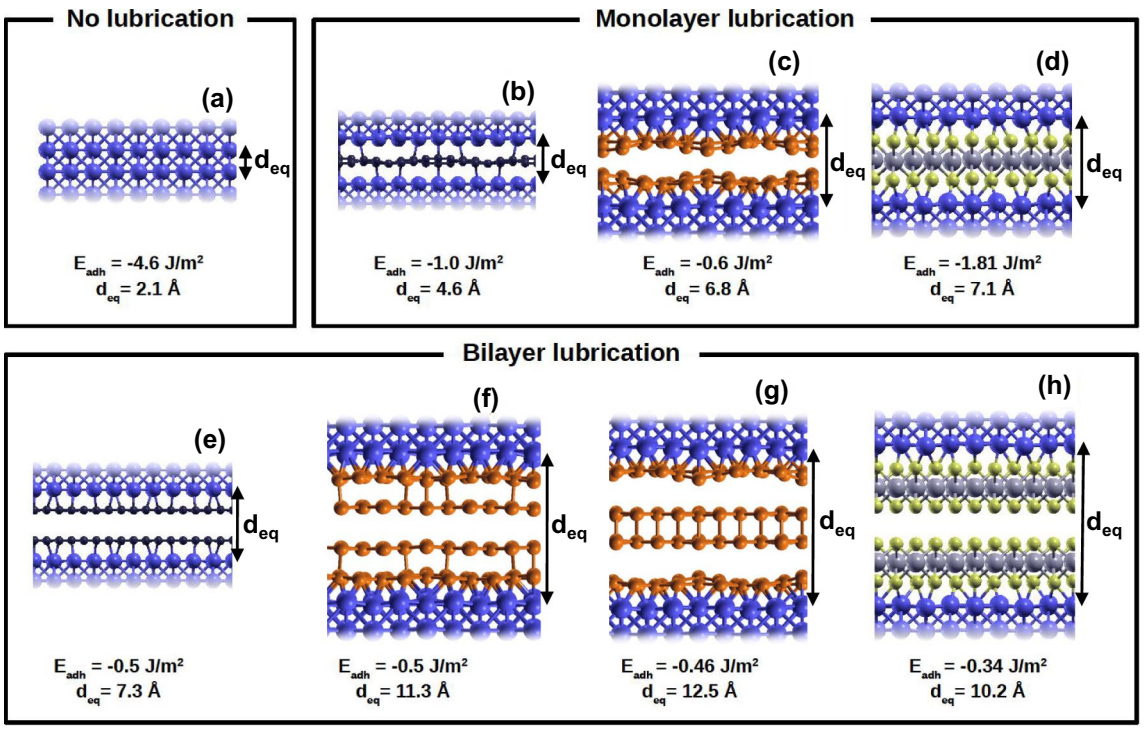

Fig. 2 The optimized structure of the interface obtained by mating two native iron surfaces (**a**) is compared with those obtained by mating a native surface with a coated substrate (**b**–**d**) and two coated surfaces (**e**–**h**). The interfacial adhesion, E_{adh}, and metal–metal separation, d_{eq}, are also reported

Table 1 Adhesion energies (in J/m^2) of the iron–iron interface intercalated with one layer and two layers of 2D materials

	One layer	Two layers
Graphene [21]	−1.0 (78%)	−0.5 (89%)
Phosphorene	−0.6 (87%)	−0.5 (89%)
MoS_2	−1.8 (61%)	−0.3 (93%)

The percentage reductions of the adhesion energy with respect to the clean iron–iron interface (−4.6 J/m^2) are reported in brackets

the chemisorbed phosphorous to interact not only with the iron substrate but also to make P–P covalent bonds. The P–P covalent bonds lead to the formation of a two-dimensional overlayer which is responsible for the reduced metal reactivity. This effect has been quantitatively described by calculating the P–P interaction energy and the projected density of states (PDOS) in a previous paper by some of us [16]. These P–P chemical bonds occur only for high concentration of P adsorbed atoms, as the cases presented in this work. The

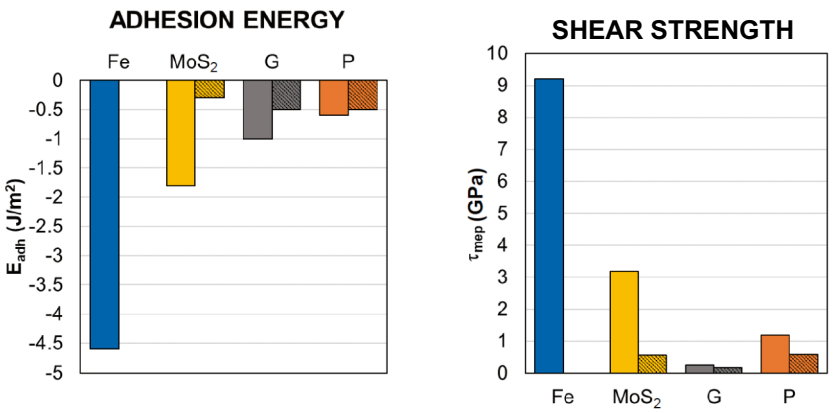

Fig. 3 Adhesion energies and shear strengths for the bare and lubricated iron interfaces. Lighter colors indicate single intercalation and darker colors indicate double intercalation

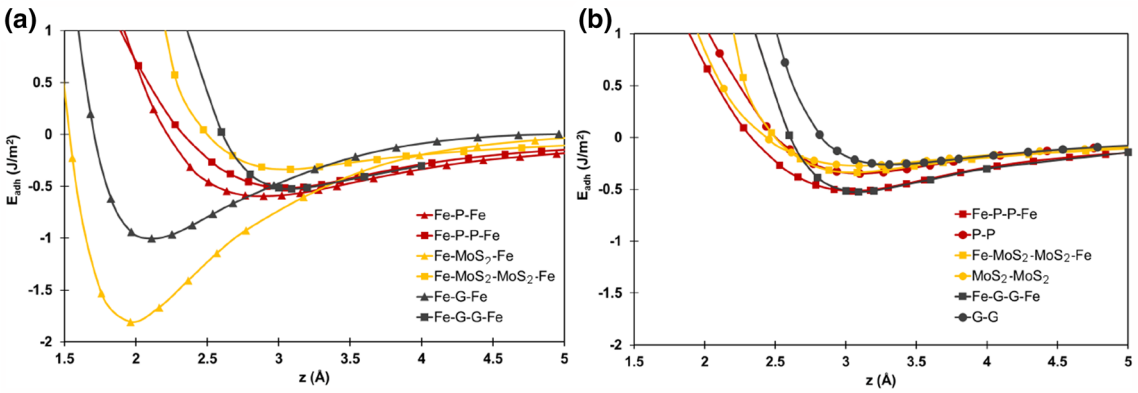

Fig. 4 Adhesion energy profile along the perpendicular direction to the interface for (**a**) single and double 2D material intercalated iron-iron interfaces, (**b**) double 2D material intercalated iron–iron interfaces and bare 2D-material/2D-material interfaces

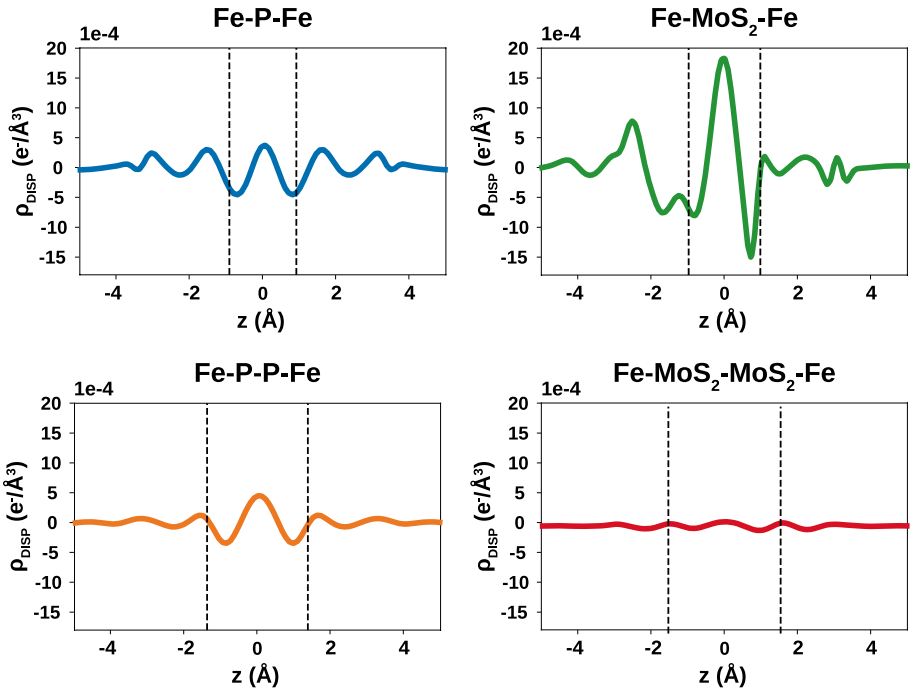

Fig. 5 Charge displacement at the interfaces under study. Dotted lines indicate the boundaries of the interfacial region. The charge redistribution is calculated by integrating the $\rho_{DISP}(z)$ curve in this interval

PDOS analysis shows a large broadening of both the 3s and 3p states of the P overlayer atoms compared to P isolated atoms. This clearly points out the existence of a P–P interaction leading to the formation of a P band. The formation of such band has the consequences of reducing the P–Fe interaction in favor of the interlayer P–P interaction. This result indicates that phosphorene has excellent potential as a solid lubricant for iron/steel in dry conditions.

The adhesion reduction of phosphorene is more pronounced than that of MoS_2 and single graphene layers, as can be seen from Fig. 3. Both MoS_2 and graphene have a passivating effect different from phosphorene. They do not break apart with an overall limited structure deformation. In this case, the coating interacts with the countersure as it interacts with the substrate, making adhesion reduction less efficient.

To get insights into the interaction between the coating and pristine countersurface, we computed the adhesion as a function of the separation of the surfaces (Fig. 4). The energy values in the minimum correspond to the adhesion values reported in Table 1. The adhesion-vs-separation curve obtained for the interface with an intercalated phosphorene layer presents a shallow minimum at a longer distance ($z > 3$ Å), indicating that the surfaces interact by weak vdW

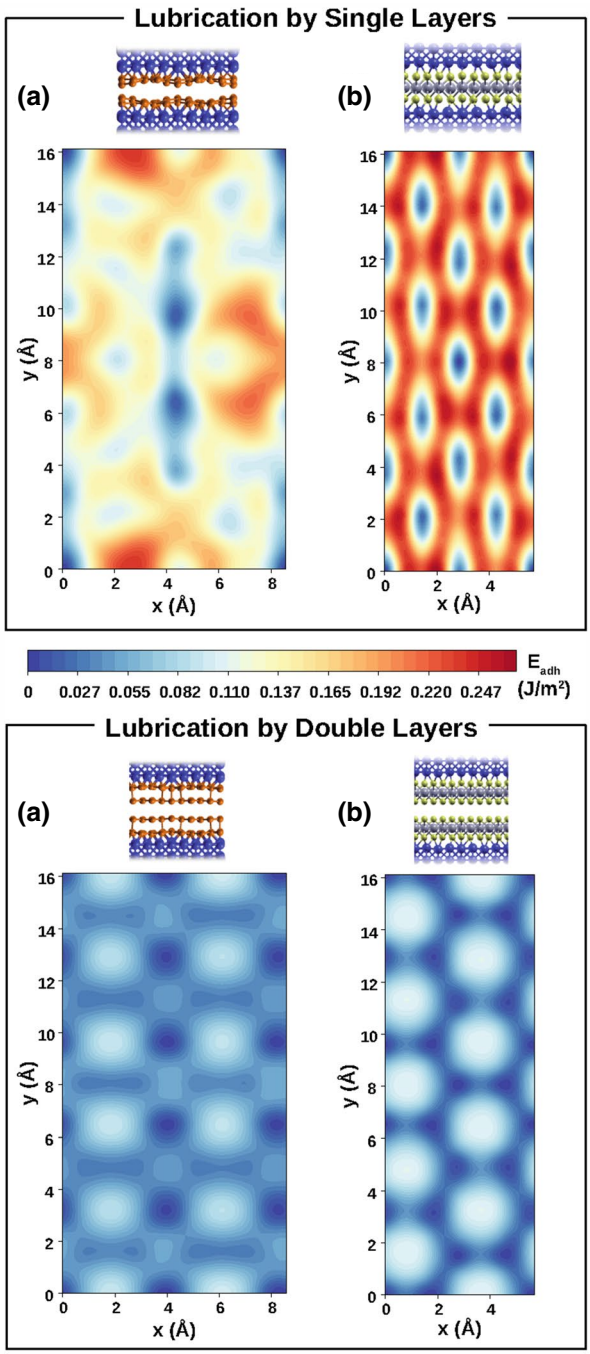

Fig. 6 Potential Energy Surface of a Fe(110)-Fe(110) interface, passivated by a monolayer of phosphorene (**a**) and MoS_2 (**b**), and by a bilayer of phosphorene (**c**) and MoS_2 (**d**), intercalated at the interface. For the sake of comparison, all the PES are represented on the same energy scale

forces. MoS_2 and graphene produce a deeper minimum located at a smaller distance ($z \sim 2$ Å), indicating the presence of chemical bonds between the 2D material and the countersurface. Only phosphorene can prevent chemical interaction across the interface at this level of coverage.

The energy of adhesion between surfaces has roots in electrons interactions. Upon interface formation, the electronic density is perturbed due to bond formation and/or electrostatic interactions. These effects induce a redistribution of the electronic charge, the amount of which is proportional to the adhesion [50]. To investigate this phenomenon, we reported the charge redistribution, i.e., the difference between the total charge of the interface and the sum of the charges of the separated surfaces, as a function of the surfaces separation, z, in Fig. 5. The larger charge redistribution occurs at the interfacial region, which is the most perturbed when the two surfaces are mated. In this region, we calculated the integral of the charge redistribution, i.e., ρ_{redist}, which is reported in Table 2. This quantity well correlates with E_{adh}, uncovering the link between the charge redistribution and adhesion [50].

We estimated the considered 2D materials capability to reduce the resistance to sliding by calculating the ideal interfacial shear stress, i.e., the static friction force per unit area. The interface failure against sliding most likely occurs along the MEP. The calculated PESes are reported in Fig. 6 of the supplementary materials, while the maximum resistance force alongside the MEP, τ_{mep}, is reported in Table 2 and Fig.3. Our results indicate that a single layer of 2D material can effectively reduce the iron sliding resistance by screening the metal–metal interaction. The presence of the coating keeps the mated iron surfaces at non-bonding distances.

We then considered two layers of material intercalated at the iron interface to mimic a lubricated contact where the solid lubricant covers both the substrate and the countersurface. In these conditions, the adhesion energies are further reduced, see Fig. 3, and the adhesion-vs-separation curves resemble those of isolated bilayers of 2D materials, see Fig. 4b. This effect is due to the full passivation of iron surfaces, with an interfacial separation of at least 7 Å and weak interaction between them. The charge redistribution occurring at the interface is strongly reduced, as well as the adhesion energy, see Fig. 5.

The adhesion reduction obtained by including a second phosphorene layer between two iron surfaces is smaller compared with MoS_2 and graphene, see Fig. 3 and Fig. 4a. Indeed, as mentioned before, thanks to its structure, a single phosphorene layer can provide two separated atomic-thin coatings to passivate almost completely both the surfaces at the interface, making the additional coating of the countersurface not necessary. The ideal shear strength τ_{mep} follows the trend of the adhesion energy. The most efficient in lubrication is graphene, with τ_{mep} equal to 0.17 GPa [21].

Table 2 Comparison of the tribological figures of merit of the selected lubricant coatings. Fe–X–Fe and Fe–X–X-Fe stand for single and double intercalation, with X = P, MoS_2 and G. P stands for Phosphorene, and G for graphene

	d_{eq} (Å)	E_{adh} (J/m^2)	ΔE_{adh} (J/m^2)	τ_{mep} (GPa)	ρ_{redist} (10^{-3} e$^-$/Å^3)
Fe–Fe	2.1	−4.60	1.60	9.20	21
Fe–P–Fe	6.8	−0.60	0.24	1.18	0.26
Fe–P–P–Fe	12.5	−0.46	0.10	0.59	0.22
Fe–MoS_2-Fe	7.1	−1.81	0.27	3.18	0.90
Fe–MoS_2-MoS_2-Fe	10.2	−0.34	0.11	0.57	0.04
Fe–G–Fe	4.6	−1.00	0.10	0.24	0.97
Fe–G–G–Fe	7.3	−0.50	0.08	0.17	0.20

Conclusion

Our results uncover promising properties of phosphorene as a solid lubricant for iron/steel. Phosphorene strongly chemisorbs on native iron surfaces, presenting higher binding energy than MoS_2 and graphene [21]. The higher the adhesion between the lubricant and the substrate, the more stable the surface passivation is, which can resist the peeling-off produced by rubbing. Furthermore, our simulations indicate that a single layer of phosphorene can passivate both the substrate and countersurface, thanks to its peculiar structure that splits into two atomic-thin layers upon intercalation. In this way, we expect phosphorene to reduce adhesion more efficiently than other well-established solid lubricants at low concentrations. The performances of phosphorene as lubricant additive have been studied in Ref. [51] and compared to those of graphene and MoS_2. The results show that at very low concentrations, phosphorene performs better than the other solid lubricants. This experimental result is in very good agreement with the outcome of our simulations.

Supplementary Information The online version contains supplementary material available at https://doi.org/10.1007/s40097-022-00478-1.

Acknowledgements These results are part of the "Advancing Solid Interface and Lubricants by First Principles Material Design (SLIDE)" project that has received funding from the European Research Council (ERC) under the European Union's Horizon 2020 research and innovation program (Grant agreement No. 865633). Furthermore, the authors acknowledge Prof. Carlo Calandra for the fruitful discussion.

Funding Open access funding provided by Alma Mater Studiorum - Università di Bologna within the CRUI-CARE Agreement.

References

1. International Energy Agency: Energy Technology Perspectives 2020 - Special report on clean energy innovation, pp. 185. OECD, (2020)
2. Holmberg, K., Erdemir, A.: Influence of tribology on global energy consumption, costs and emissions. Friction **5**, 263–284 (2017)
3. Spear, J.C., Ewers, B.W., Batteas, J.D.: 2D-nanomaterials for controlling friction and wear at interfaces. Nano Today **10**, 301–314 (2015)
4. Elinski, M.B., Liu, Z., Spear, J.C., Batteas, J.D.: 2D or not 2D? The impact of nanoscale roughness and substrate interactions on the tribological properties of graphene and MoS2. J. Phys. D Appl. Phys. **50**, 103003–314 (2017)
5. Rosenkranz, A., Liu, Y., Yang, L., Chen, L.: 2D nano-materials beyond graphene: from synthesis to tribological studies Appl. Nanoscience **10**, 3353–3388 (2020)
6. Wu, S., He, F., Xie, G., Bian, Z., Ren, Y., Liu, X., Yang, H., Guo, D., Zhang, L., Wen, S., Luo, J.: Super-slippery degraded black phosphorus/silicon dioxide interface. ACS Appl. Mater. Interfaces **12**, 7717–7726 (2020)
7. Wu, S., He, F., Xie, G., Bian, Z., Luo, J., Wen, S.: Black phosphorus: degradation favors lubrication. Nano Lett. **18**, 5618–5627 (2018)
8. Cui, Z., Xie, G., He, F., Wang, W., Guo, D., Wang, W.: Atomic-scale sriction of black phosphorus: effect of thickness and anisotropic behavior. Adv. Mater. Interf. **4**, 1–9 (2017)
9. Galluzzi, M., Zhang, Y., Yu, X.-F.: Mechanical properties and applications of 2D black phosphorus. J. Appl. Phys. **128**, 230903 (2020)
10. Wang, W., Xie, G., Luo, J.: Superlubricity of black phosphorus as lubricant additive. ACS Appl. Mater. Interfaces **10**, 43203–43210 (2018)
11. Losi, G., Restuccia, P., Righi, M.C.: Superlubricity in phosphorene identified by means of ab initio calculations. 2D Mater. 7, 025033 (2020)
12. De Barros-Bouchet, M.I., Righi, M.C., Philippon, D., Mambingo-Doumbe, S., Le-Mogne, T., Martin, J.M., Bouffet, A.: Tribochemistry of phosphorus additives: experiments and first-principles calculations. RSC Adv. **5**, 49270–49279 (2015)
13. Righi, M.C., Loehlé, S., De Barros Bouchet, M.I., Mambingo-Doumbe, S., Martin, J.M.: A comparative study on the

functionality of s- and p-based lubricant additives by combined first principles and experimental analysis. RSC Adv. **6**, 47753–47760 (2016)
14. Loehlé, S., Righi, M.C.: Ab initio molecular dynamics simulation of tribochemical reactions involving phosphorus additives at sliding iron interfaces Lubricants **6**, 31 (2018)
15. Loehlé, S., Righi, M.C.: First principles study of organophosphorus additives in boundary lubrication conditions: effects of hydrocarbon chain length. Lubr. Sci. **29**, 485–491 (2017)
16. Fatti, G., Restuccia, P., Calandra, C., Righi, M.C.: Phosphorus adsorption on fe(110): an ab initio comparative study of iron passivation by different adsorbates. J. Phys. Chem. C **122**, 28105–28112 (2018)
17. De Barros Bouchet, M.I., Martin, J.M., Le Mogne, T., Bilas, P., Vacher, B., Yamada, Y.: Mechanisms of mos2 formation by modtc in presence of zndtp: effect of oxidative degradation. Wear **258**, 1643–1650 (2005)
18. Martin, J.-M., Grossiord, C., Mogne, T.L., Igarashi, J.: Transfer films and friction under boundary lubrication. Wear **245**, 107–115 (2000)
19. Losi, G., Peeters, S., Delayens, F., Vezin, H., Loehlé, S., Thiebaut, B., Righi, M.C.: Experimental and ab initio characterization of mononuclear molybdenum dithiocarbamates in lubricant mixtures. Langmuir **37**, 4836–4846 (2021)
20. Marchetto, D., Restuccia, P., Ballestrazzi, A., Righi, M.C., Rota, A., Valeri, S.: Surface passivation by graphene in the lubrication of iron: A comparison with bronze. Carbon **116**, 375–380 (2017)
21. Restuccia, P., Righi, M.C.: Tribochemistry of graphene on iron and its possible role in lubrication of steel. Carbon **106**, 118–124 (2016)
22. Berman, D., Erdemir, A., Sumant, A.V.: Graphene: a new emerging lubricant. Mater. Today **17**, 31–42 (2014)
23. Berman, D., Erdemir, A., Sumant, A.V.: Few layer graphene to reduce wear and friction on sliding steel surfaces. Carbon **54**, 454–459 (2013)
24. Berman, D., Erdemir, A., Sumant, A.V.: Reduced wear and friction enabled by graphene layers on sliding steel surfaces in dry nitrogen. Carbon **59**, 167–175 (2013)
25. Giannozzi, P., Baroni, S., Bonini, N., Calandra, M., Car, R., Cavazzoni, C., Ceresoli, D., Chiarotti, G.L., Cococcioni, M., Dabo, I., Corso, A.D., de Gironcoli, S., Fabris, S., Fratesi, G., Gebauer, R., Gerstmann, U., Gougoussis, C., Kokalj, A., Lazzeri, M., Martin-Samos, L., Marzari, N., Mauri, F., Mazzarello, R., Paolini, S., Pasquarello, A., Paulatto, L., Sbraccia, C., Scandolo, S., Sclauzero, G., Seitsonen, A.P., Smogunov, A., Umari, P., Wentzcovitch, R.M.: Quantum espresso: a modular and open-source software project for quantum simulations of materials. J. Phys. Condens. Matter. **21**, 395502 (2009)
26. Giannozzi, P., Andreussi, O., Brumme, T., Bunau, O., Nardelli, M.B., Calandra, M., Car, R., Cavazzoni, C., Ceresoli, D., Cococcioni, M., Colonna, N., Carnimeo, I., Corso, A.D., de Gironcoli, S., Delugas, P., Jr., R.A.D., Ferretti, A., Floris, A., Fratesi, G., Fugallo, G., Gebauer, R., Gerstmann, U., Giustino, F., Gorni, T., Jia, J., Kawamura, M., Ko, H.-Y., Kokalj, A., Küçükbenli, E., Lazzeri, M., Marsili, M., Marzari, N., Mauri, F., Nguyen, N.L., Nguyen, H.-V., Otero-de-la-Roza, A., Paulatto, L., Poncé, S., Rocca, D., Sabatini, R., Santra, B., Schlipf, M., Seitsonen, A.P., Smogunov, A., Timrov, I., Thonhauser, T., Umari, P., Vast, N., Wu, X., Baroni, S.: Advanced capabilities for materials modelling with quantum espresso. J. Phys. Condens. Matter. **29**, 465901 (2017)
27. Vanderbilt, D.: Soft self-consistent pseudopotentials in a generalized eigenvalue formalism. Phys. Rev. B **41**, 7892–7895 (1990)
28. Perdew, J.P., Burke, K., Ernzerhof, M.: Generalized gradient approximation made simple. Phys. Rev. Lett. **77**, 3865–3868 (1996)
29. Grimme, S.: Semiempirical gga-type density functional constructed with a long-range dispersion correction. J. Comput. Chem. **27**, 1787–1799 (2006)
30. Cutini, M., Corno, M., Ugliengo, P.: Method Dependence of Proline Ring Flexibility in the Poly-L-Proline Type II Polymer. J. Chem. Theory Comput. **13**, 370–379 (2017)
31. Cutini, M., Bocus, M., Ugliengo, P.: Decoding collagen triple helix stability by means of hybrid DFT simulations. J. Phys. Chem. B **123**, 7354–7364 (2019)
32. Cutini, M., Bechis, I., Corno, M., Ugliengo, P.: Balancing cost and accuracy in quantum mechanical simulations on collagen protein models. J. Chem. Theory Comput. **17**, 2566–2574 (2021)
33. Cutini, M., Pantaleone, S., Ugliengo, P.: Elucidating the nature of interactions in collagen triple-helix wrapping. J. Phys. Chem. Lett. **10**, 7644–7649 (2019)
34. Cutini, M., Ugliengo, P.: Infrared harmonic features of collagen models at B3LYP-D3: from amide bands to the thz region. J. Chem. Phys. **155**, 075102 (2021)
35. Cutini, M., Corno, M., Costa, D., Ugliengo, P.: How does collagen adsorb on hydroxyapatite? Insights from Ab initio simulations on a polyproline type II model. J. Phys. Chem. C **123**, 7540–7550 (2019)
36. Cutini, M., Civalleri, B., Ugliengo, P.: Cost-effective quantum mechanical approach for predicting thermodynamic and mechanical stability of pure-silica Zeolites. ACS Omega **4**, 1838–1846 (2019)
37. Ilawe, N.V., Zimmerman, J.A., Wong, B.M.: Breaking badly: DFT-D2 gives sizeable errors for tensile strengths in palladium-hydride solids. J. Chem. Theory Comput. **11**, 5426–5435 (2015)
38. Shao, L., Ye, H., Wu, Y., Yinxiao, D., Ding, P., Zeng, F., Yuan, Q.: Interaction between phosphorene and the surface of a substrate. Mater. Res. Express. **3**, 025013 (2016)
39. Shulenburger, L., Baczewski, A.D., Zhu, Z., Guan, J., Tománek, D.: The nature of the interlayer interaction in bulk and few-layer phosphorus. Nano Lett. **15**, 8170–8175 (2015)
40. Levita, G., Cavaleiro, A., Molinari, E., Polcar, T., Righi, M.C.: Sliding properties of MoS2 layers: load and interlayer orientation effects. J. Phys. Chem. C **118**, 13809–13816 (2014)
41. Levita, G., Molinari, E., Polcar, T., Righi, M.C.: First-principles comparative study on the interlayer adhesion and shear strength of transition-metal dichalcogenides and graphene. Phys. Rev. B **92**, 085434 (2015)
42. Levita, G., Restuccia, P., Righi, M.C.: Graphene and MoS2 interacting with water: a comparison by ab initio calculations. Carbon **107**, 878–884 (2016)
43. Wolloch, M., Losi, G., Ferrario, M., Righi, M.C.: High-throughput screening of the static friction and ideal cleavage strength of solid interfaces. Sci. Rep. **9**, 17062 (2019)
44. Fantauzzi, M., Secci, F., Sanna Angotzi, M., Passiu, C., Cannas, C., Rossi, A.: Nanostructured spinel cobalt ferrites: Fe and co chemical state, cation distribution and size effects by x-ray photoelectron spectroscopy. RSC Adv. **9**, 19171–19179 (2019)
45. Peeters, S., Charrin, C., Duron, I., Loehlé, S., Thiebaut, B., Righi, M.C.: Importance of the catalytic effect of the substrate in the functionality of lubricant additives: the case of molybdenum dithiocarbamates. Mater. Today Chem. **21**, 100487 (2021)
46. Restuccia, P., Levita, G., Wolloch, M., Losi, G., Fatti, G., Ferrario, M., Righi, M.C.: Ideal adhesive and shear strengths of solid interfaces: a high throughput ab initio approach. Comput. Mater. Sci. **154**, 517–529 (2018)
47. Zilibotti, G., Righi, M.C.: Ab initio calculation of the adhesion and ideal shear strength of planar diamond interfaces with different atomic structure and hydrogen coverage. Langmuir **27**, 6862–6867 (2011)

48. E, W., Ren, W., Vanden-Eijnden, E.: Simplified and improved string method for computing the minimum energy paths in barrier-crossing events. J. Chem. Phys. 126, 164103 (2007)
49. Pan, Y., Wang, Y., Ye, M., Quhe, R., Zhong, H., Song, Z., Peng, X., Yu, D., Yang, J., Shi, J., Lu, J.: Monolayer phosphorene-metal contacts. Chem. Mater. **28**, 2100–2109 (2016)
50. Wolloch, M., Levita, G., Restuccia, P., Righi, M.C.: Interfacial charge density and its connection to adhesion and frictional forces. Phys. Rev. Lett. **121**, 026804 (2018)
51. Wang, W., Xie, G., Luo, J.: Black phosphorus as a new lubricant. Friction **6**, 116–142 (2018)